CLM - R 144

CLM - R 144

UKAEA RESEARCH GROUP

Report

TRANSIT TIME MAGNETIC PUMPING EXPERIMENTS IN THE PROTO-CLEO STELLARATOR

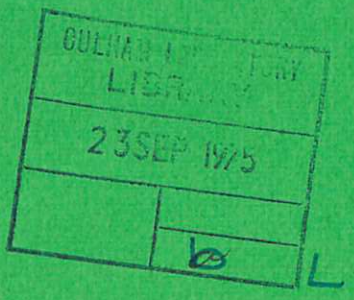

W. MILLAR

CULHAM LABORATORY
Abingdon Oxfordshire
1975

Available from H. M. Stationery Office

C.18

PRICE 50p

CONTENTS

1. INTRODUCTION

In transit time magnetic pumping (TTMP), the confining magnetic field is perturbed by adding a wave, or waves, of the form $\cos(\omega t - kz)$, where z is the direction both of the confining and of the wave field. Here we consider a standing wave $B_1 \sin \omega t \sin kz$. Then for the heating rate $1/\tau$, defined as $\frac{d(n\,T_i)}{dt} / (nT_i)$, of a plasma in the field, TTMP theory[1] gives

$$1/\tau = \omega b^2 x \exp(-x^2) \cdot \sqrt{\pi}/3 \qquad ..(1)$$

where

$$\left.\begin{aligned} b &= B_1/B_o \\ x &= v_{phase}/v_{thermal} \\ v_{phase} &= \omega/k \\ v_{thermal} &= \sqrt{2\,K\,T_i/m_i} \end{aligned}\right\} \qquad ..(2)$$

Equation (1) gives a maximum with $x = 1/\sqrt{2}$, when

$$1/\tau = 0.253\ \omega b^2 \ . \qquad ..(3)$$

For the full amount of heating, the plasma density must exceed a certain value n_{crit}, given roughly, for $x = 1/\sqrt{2}$, by

$$n_{crit} = 3.7 \times 10^5\ T_i^{\frac{3}{2}}\ \omega b^{\frac{3}{2}},\ T_i \text{ in eV}. \qquad ..(4)$$

A more precise treatment of critical density is given by Cannobbio[2]. In deriving Eqn.(1) it has been assumed that all the TTMP energy is retained by the ions. Also the above theory neglects the effect of electron pressure, and is applicable for $T_e \ll T_i$. The effect is included by Dawson and Unman[3], who work out the case $T_e = T_i$ in detail.

This report describes an experiment in which TTMP fields were applied to the toroidal stellarator, PROTO-CLEO[4,5]. Here there are two important constraints on the TTMP parameters. Firstly, the need for an integral number, m, of waves round the torus requires

$$k = m/R \qquad ..(5)$$

where R is the major radius. Secondly, a significant heating experiment should have $\tau \leq \tau_E$, the energy confinement time. Putting $R = 40$ cm as in PROTO-CLEO, and $T_i = 10$ eV, Eqns (2) and (5) with $x = 1/\sqrt{2}$ give, for H ions,

$$\omega = 7.77 \times 10^4 m \ . \qquad ..(6)$$

Putting $\tau = 2.5$ ms, which is a typical value for τ_E in PROTO-CLEO, gives with Eqns.(2)-(5)

$$b = 0.143\ m^{-\frac{1}{2}} \qquad ..(7)$$

and

$$n_{crit} = 4.9 \times 10^{10}\ m^{\frac{1}{4}} \quad . \qquad ..(8)$$

Table I shows the resulting values of $f(=\omega/2\pi)$, b, and n_{crit}, for the cases m = 7,3,2 and 1. Also shown in this table are estimates of the current, voltage, power loss in the coils and tuning capacity to set up the required fields; these estimates are explained in Section 2. For m = 3,2 and 1 it is assumed that the TTMP field is uniform across the plasma, since $\nu_p \ll 1/k$. For m = 7 a small correction is included. Note that the table shows the parameters for a heating time of 2.5 ms, and is based on the parameters R = 40 cm, T_i = 10 eV, x = 1//2, hydrogen ions. TTMP operates for $n_{crit} \lesssim n \lesssim 10^{13}\ cm^{-3}$; at higher density, collisional heating takes over.

TABLE I

CALCULATED PARAMETERS FOR A HEATING TIME OF 2.5 ms
WITH T_i = 10eV, x = 1//2, H^+ IONS

MODE NUMBER m	7	3	2	1	UNITS
Modulation b	5.4	8.2	9.9	14.3	%
TTMP frequency f	86.5	37.1	24.7	12.4	kHz
Critical density n_{crit}	8.2	6.5	5.9	4.9	$\times 10^{10}\ cm^{-3}$
Coil Current	1.24	1.59	1.61	2.02	kA
Total Coil Power	235	215	180	200	kW
Volts to Ground	1070	590	400	250	Volt
Capacity per Coil	1.0	5.4	12.3	49	μF

The experiments which were carried out are described in Section 3. All were dominated by plasma pump-out effects, consistent with a modified stellarator diffusion theory due to Stringer[6]. The pump-out was so great that there was no hope of being able to increase the plasma energy content by TTMP. With restricted modulation, a decrease in the plasma cooling rate, of the right order for TTMP, was indeed observed. The same effect however occurred with a high-f low-m combination, where TTMP is negligible; the heating experiments were therefore inconclusive. The pump-out rate was studied as a function of m, f, b and other parameters, in the hope that the results might help to explain the

pump-out mechanism. For the lower values of m , the frequencies used were actually much too high for TTMP, and there is therefore a gap in the investigation. It is quite possible, for all one can say here, that pump-out could be much less severe when using the modes m = 1 or m = 2, with their appropriate frequencies as in Table I, in spite of the higher b values required.

The RF electric field in these experiments is of some importance. Taking first the vacuum field, it satisfies

$$\text{curl } \underline{E} = -\frac{1}{c} \cdot \frac{\partial \underline{B}}{\partial t} \quad .$$

It is usual to take $\underline{E} = \underline{E}_1 + \underline{E}_2$, where $\underline{E}_1$ is a simple solution which is zero on some convenient axis, in this case the minor axis of the torus. $\underline{E}_2$ is the electrostatic component, strongly dependent on the boundary conditions. In this experiment the boundary consists mainly of the coils and the helical winding. It is possible in principle to make $|\underline{E}_2| \ll |\underline{E}_1|$, and an attempt to do so by means of a Faraday cage is described at the end of Section 2. The question of the electric field in the presence of plasma is more difficult. Although on a simple picture one would expect the outer layers of the plasma to screen out electrostatic fields, the situation is complicated by the presence of a magnetic field, by the fact that the plasma boundary is not sharp, and by the possible existence of plasma waves which can couple to external fields. Evidence for pump-out by purely electrostatic RF fields is given in Section 3.2.

Reference to Table I will show that, at plasma densities $\sim 10^{11}\,\text{cm}^{-3}$ the power given to the plasma by TTMP is very small. Under reactor conditions, however, where the plasma pressure would be several orders of magnitude greater and the coils physically larger and of better proportions, the plasma power would exceed the coil power.

2. DESCRIPTION

PROTO-CLEO has been fully described elsewhere[4,5]. To set up the TTMP fields discussed in Section 1, a number of additional coils were fitted. A section through the torus, with its ℓ = 2 winding, is illustrated in Fig. 1, which also shows a typical section of the plasma as determined by the magnetic separatrix. Outside that surface, the plasma density is low but not zero. Because there was a danger that the presence of RF coils placed in this low density region might precipitate an electrical breakdown between different parts of the un-insulated helical winding, the new coils were fitted outside the helical winding. Fig. 2 shows a plan view of that winding and its supports, which consist of 15 fixed and equispaced ceramic rings. There are thus 15 possible coil sites between the rings. A 3-turn coil was placed in each of 14 of these sites, the

15th being required for microwave experiments. One of these coils is shown in Fig. 2. They were wound in copper tubing of diameter 6.5 mm, on a mean radius of 110 mm. The surface of the tubing was covered by Kaptan tape, which was then heated to form an insulating layer. The ends of the tubing were brought out through seals in the base of the vacuum tank, and water cooling was provided.

By energising the coils in the manner shown in Table II, it was possible to obtain field distributions approximating to the modes m = 0,1,2,3 and 7, the first of these being the uniform mode. The symbols in Table II indicate the direction of current in the coils.

TABLE II

CURRENT DIRECTIONS IN EACH COIL FOR VARIOUS MODES

COIL NUMBER	1	2	3	4	5	6	7	8	9	10	11	12	13	14	15
Mode number, m															
0	+	+	+	+	+	+	+	+	+	+	+	+	+	+	0
1	+	+	+	+	+	+	0	0	-	-	-	-	-	-	0
2	+	+	+	-	-	-	0	0	+	+	+	-	-	-	0
3	+	+	-	-	+	+	0	0	-	-	+	+	-	0	0
7	+	-	+	-	+	-	+	-	+	-	+	-	+	-	0

Because of the occurrence of zeros in Table II, none of these modes were true; strictly speaking all the distributions were sums of harmonics of m = 1 modes (and, in the first case, m = 0). For example in the arrangement defined by the last row of Table II, the seventh and eighth harmonics of m = 1 are dominant, and it can be shown by Fourier analysis that the TTMP heating effect is almost exactly the same as if we had used 14 coils equally spaced round the torus so as to give a true m = 7 mode.

The estimates of RF requirements, quoted in Table I of Section 1 were obtained by the following argument. The coils were wound on a toroidal surface of major, minor radii R,a. Since $R \gg a$ we will not be too much in error if we suppose that this toroidal surface is straightened out to form a cylinder of radius a and length $2\pi R$. We take axial, radial co-ordinates z, r. Next we suppose that for m = 7 there are 14 equally spaced coils, with the current concentrated at the centre position of each coil, while for m = 3,2 or 1 we suppose that there are 12 equally spaced coils, with the total current in each group of like-signed coils spread out over a distance $\pi R/m$ in the z-direction. That is, we take a sheet current i(z) given for m = 7 by

$$i(z) = (-1)^j I\,\delta(z-z_j), \quad z_j = j\pi/k \qquad ..(9)$$

where $j = 0,1,2 \ldots\ldots 12$ and $k = 7/R$;

and for $m = 3,2$ or 1 by .

$$i(z) = \begin{cases} 6Ik/(\pi m) , & \cos kz > 0 \\ -6Ik/(\pi m) , & \cos kz < 0 \end{cases} , \quad k = m/R \qquad ..(10)$$

where I is the equivalent single-turn current in each coil.

We need consider only the fundamental Fourier component $i_1 \cos kz$ of $i(z)$, since the harmonics do not contribute appreciably to the heating by TTMP. By standard methods we find

$$i_1 = \begin{cases} \frac{2}{\pi} \cdot Ik , & m = 7 \\ \frac{24}{\pi^2} \cdot \frac{Ik}{m} , & m = 3,2 \text{ or } 1. \end{cases} \qquad ..(11)$$

On solving Laplace's equation with the appropriate boundary conditions, the fundamental component $B_1(r) \cos kz$ of the axial magnetic field is found to be given by

$$B_1(r) = -4\pi i_1 \cdot ka \cdot K_1(ka)\, I_o(kr) , \qquad ..(12)$$

in which K_1 and I_o are the Bessel functions. In fact $I_o(kr)$ is close to unity throughout the region $r < r_{plasma}$, and is exactly unity on the axis $r = 0$. The modulation b is defined by

$$b = B_1(0)/B_o ,$$

and hence when b, k and a are specified, the required currents I are determined by Eqns. (11) and (12). The currents quoted in Table I follow on putting $R = 40$ cm, $a = 11$ cm. The current for a 3-turn coil, in amperes, is of course $10I/3$. Having calculated the currents, the other quantities are obtained from the measured inductance ($\sim 3\mu H$) and measured Q-value ($\sim\sqrt{f/10}$) of the coils, neglecting the effects of mutual inductance. The voltage quoted in Table I is one half of the voltage across the 3-turn coil, and is thus the voltage to ground if the coils are balanced.

The coils were driven by a pulsed triode oscillator, the basic circuit of which is shown in Fig.3. C_1 is a 20 kJ storage bank. V_1 is a series modulator thyratron. A second thyratron was used to end the pulse. C_2 carries the RF current. V_2 is a water-cooled triode, CAT 27, giving up to 400 kW of RF output. Its anode is connected to the ferrite-cored output transformer T_1 through the capacitor C_4, whose reactance is chosen roughly to cancel that of the leakage inductance of T_1. The output of T_1, at an impedance level $\sim 10\Omega$, is taken through the long low-impedance cable Z_1 and the

balancing ransformer T_3 to the distribution points A,B. The grid drive is also taken from the output of T_1, through T_2. C_5, R_1 provide grid bias for V_2. Each of the 14 TTMP coils L_2 is shunted with its own resonating capacitor assembly C_6, and the resulting parallel tuned circuit is connected, by one of 14 lengths of balanced twin cable, to the points AB, which are located centrally underneath the stellarator. One only of these parallel tuned circuits is earthed, at the centre point of C_6; this was found to be sufficient to ensure good balancing of all 14 coils. The coupling between the anode of V_2 and the 14 coils is quite tight, and the frequency of oscillation is determined mainly by the coils and their resonating capacitors. Nevertheless some adjustment of C_3 and C_4 was found to be necessary, for optimum performance.

The capacitor assemblies C_6 were specially built to handle the large circulating currents. Each assembly consisted of eight units of 2.1 μF at 500 V (RF), which could be connected in various series-parallel combinations. The units were dry extended-foil windings of aluminium foil with polypropylene dielectric. The windings were supplied in the unterminated state by BICC Ltd. Fig. 4 shows the winding and termination pieces ready for assembly. The fluted surfaces of the copper end plates are lightly smeared with vaseline, and are then pulled strongly towards each other by tightening the nuts on the central rod, thus squashing the projecting ends of the aluminium foils into an almost solid mass. The rubber bung ensures that the end plates remain under pressure, and also acts an an insulator.

Two sets of tests were carried out on the capacitor units. The small amplitude power factor was measured at a frequency of 120 kHz, and found to be 7×10^{-4}. This was done by inserting the unit in a coaxial structure, 2 m long and 1 m diameter, in which the copper losses were calculable and of the same order of magnitude as the capacitor loss. The power factor was measured by a resonance method. The equivalent series resistance of the capacitor units, corresponding to the above power factor, is as low as 0.2 mΩ at each end. Even so the losses are several times greater than can be accounted for in terms of the power factor of the dielectric itself, and skin effect resistance in the end plates. Calculations show that the ohmic losses in the operative parts of the foils (due both to series current and to eddy current) is negligible at the frequency used. It is probable that most of the loss occurs in the squashed foil region. Further calculations show that it should be possible to increase the capacity by a factor of ten without much effect on the power factor at 120 kHz, by increasing the outer diameter of the winding and using larger end plates.

Secondly, the capacitors were given a life test with repeated RF pulses of

duration 5 ms, frequency 120 kHz, and amplitude 700 V zero to peak. The temperature rise of the capacitors during these tests was very small, and it was deduced that the power factor had not substantially increased above its small amplitude value. The life of each of the four units tested exceeded 3000 pulses; some degradation of the dielectric near the foil edges was visible at that stage. Further tests showed that the life at 500 V was very much greater. Some tests on dielectric samples immersed in oil made it seem probable that the working voltage could be at least doubled by immersion, but this technique was not pursued because of the difficulties of designing a low-resistance termination for oil-filled windings.

The Faraday cage referred to in Section 1 consisted of 36 bare copper wires of diameter 2.2 mm, mounted just inside the helical winding. A section through the helical winding and cage is shown in Fig. 5. The wires of the cage were all parallel to the minor axis. They did not pass quite completely round the torus; a short gap was left as shown in Fig. 6a, and a pair of twisted leads passing through a vacuum seal, was provided so that the gap could be shorted out externally. The purpose of this arrangement was to permit experiments on toroidal plasma currents. It will be noticed that the copper rings which join all the wires on each side of the gap have themselves a gap in minor azimuth, so as not to spoil the uniformity of the m = 0 RF mode (Fig. 6b).

3. EXPERIMENTAL RESULTS

Most of the experiments described here were investigations of the plasma pump-out effect mentioned in Section 1, together with an inconclusive search for a TTMP heating effect. All the experiments had $\ell=2$, and unless otherwise stated the confining field, B_ϕ, was 3.0 kG, the rotational transform, ι, was 0.35 at the centre, and the Faraday cage was in position.

3.1 Effects of amplitude, frequency, and wave-number

Figure 7 shows the pump-out rate $1/\tau_1$ in the m = 7 mode, as a function of the modulation b, for three different frequencies. The loss rate without RF($\sim 0.2\ ms^{-1}$) has been allowed for, so all curves pass through the origin. Most points in Fig. 7 represent the mean of three or more shots, and the standard deviation is shown by error bars. The electron density was measured with a 16 mm microwave interferometer, and is a line average. Taking n_1 and n_2 as the densities in two shots, the first with and the second without modulation, plots of the quantity $[\log n_1(t) - \log n_2(t)]$ were always found to give a good straight line over a region in which the density decayed by a factor 5 or more, even in cases where the separate plots of $\log n_1(t)$ and $\log n_2(t)$ showed some curvature. The

slope of this straight line was taken to be the loss rate due to RF modulation. For these results the density was $\sim 5 \times 10^{10}$ cm^{-3} at the beginning of the straight part. Plasma temperatures were not measured simultaneously, but under comparable conditions T_i was in the range 10 - 20 eV, and T_e in the range 2 - 4 eV. Fig. 8 shows some typical interferometer traces, and Fig. 9 shows a set of plots of $[\log n_1(t) - \log n_2(t)]$ used in obtaining Fig.7.

In summary the results show an approximately linear dependence of loss rate on modulation, with no sign of a threshold amplitude for the onset of pump-out. It should be remembered however that the loss rate is defined in a special way, and at small b is less than the unmodulated loss rate.

Fig. 10 shows the variation of loss rate with mode number m, which was varied as described in Section 2. The frequency here was 120 kHz, and the b value 2.5% in each case. For the uniform mode (m = 0), b is defined to be B'/B_0 where B' is the value of the RF field on the axis. Thus for the same b there is twice as much stored energy in the RF field for m = 0 as for m > 0. Unfortunately there are no measurements at lower frequencies; it would have been of interest to go down to about 10 kHz.

3.2 Electrostatic effects

A number of results on RF pump-out in PROTO-CLEO, without the Faraday cage, were reported previously[7]. At a later date, when the vacuum tank was opened up in order to insert the cage, it was discovered that two of the coils, numbers 3 and 7, were connected in the opposite direction to that intended. This is unlikely to affect the general conclusions of the previous report, but it does mean that care is required in comparing results with and without the cage. A direct measure of the effect of the cage was obtained by setting up the coil connections as for m = 7, but with coils 3 and 7 reversed. The RF conditions were then exactly as in the original experiment, except that the Faraday cage was now in position. It was found that the RF loss rate with the cage was 0.36 times that without, a result which gives weight to the supposition that the electrostatic field ($\underline{E}_2$ in Section 1) is playing some part in the pump-out mechanism. Further support for this idea comes from two other observations:

1. Without the cage, one terminal of each of the odd-numbered coils was connected to the point A (Figure 3), the other terminal being open-circuit. Similarly one terminal of each of the even-numbered coils was connected to the point B. The system was balanced in the usual manner so that the potentials at A and B with respect to ground were 180° out of phase, the values being 1200 V with

respect to ground in each case. The frequency was 124 kHz. The perturbation of magnetic field produced by this arrangement was completely negligible, but the electric field near the coils was comparable in magnitude (though of different geometry) to the electrostatic field in the normal case with the coils carrying the currents appropriate to b = 3.75%, where the voltage to ground from either terminal of the coil is again 1200 V. RF pump-out was observed in the first case; the rate was about $\frac{1}{10}$ of that in the second (using linear extrapolation beyond b = 2.5%), and therefore about $\frac{1}{3}$ of that in the corresponding case with the cage in position. This result is quite striking, since it shows that RF pump-out can be produced by purely electrostatic means.

2. Measurable RF pump-out was produced when a voltage of 800 V at f = 177 kHz was applied between the cage and the wall of the vacuum tank. This is another instance of purely electrostatic pump-out, and also shows that the cage was not a perfect electrostatic screen.

It was not possible to reduce the screening effect of the cage by removing the external short on the twisted enamel wires, C in Figure 6a, because the capacity between the two wires of the pair greatly exceeded the self capacity of the cage.

3.3 Density dependence

The RF pump-out rate did not change substantially with density over the range 3×10^{9} to $1 \times 10^{12}\,cm^{-3}$. The accuracy of the measurement was limited at low densities by background noise and at high densities by ambiguities in interpreting interferometer fringes. It was clear however that the RF loss rate at high densities was great enough to exclude the loss disc instability as a possible pump-out mechanisam.

3.4 Transform dependence

Figure 11 shows the effect of reducing the rotational transform. The quantity plotted is the overall confinement time, $\tau' = n/\frac{dn}{dt}$. The measurement is taken 2 ms after gun injection except where the confinement time is short, when the time delay is smaller. At any one transform value, the measurements with and without RF had the same time delay. The values of ι refer to the minor axis, and are obtained from computer plots of transform as a function of helical winding current. The confining field was 3.0 kG and the plasma density $\sim 5 \times 10^{10}$ in these measurements.

The effect of increasing the transform to values greater than 0.35 was also investigated. To do this it was necessary to reduce the confining magnetic field B_{ϕ}. The resulting confinement times were broadly consistent with the plasma volume as calculated

from the computed separatrix, taking the change in B_ϕ and ϵ into account. There was no marked change in the effect of RF as the plasma moved inwards; this disposes of the possibility that the RF pump-out might be associated with the proximity of the plasma to the cage.

3.5. Langmuir probe measurements

Measurements were made by D.J. Lees of the plasma profile during the application of the RF pulse, using a Langmuir probe. It was found that the shape and size of the plasma remained constant, despite an order of magnitude reduction in density due to RF pump-out. Lees also examined the fluctuations in floating potential ($\tilde{V}_f$) and in azimuthal electric field ($\tilde{E}_\phi$), using filters to confine the observation of fluctuations to the frequency region 1 - 30 kHz. Both $\tilde{V}_f$ and $\tilde{E}_\phi$ increased by a factor ~ 3 when modulation (m = 7, f = 120 kHz, b = 2.5%) was applied, but there was no marked change in the character of the fluctuations.

3.6 Modulation in space only

Steady currents were set up in the TTMP coils from a DC generator, to produce a modulation with m = 7, f = 0, b = 2.5%. No decrease in confinement time could be observed. Thus one does not look to break-up of the magnetic surfaces as a cause of pump-out. It has also been shown by field computations that perturbations of the above type and magnitude should not break up the magnetic surfaces.

3.7 Heating effects

With a modulation of 2.5% the TTMP heating is not great enough to produce an increase in the ion temperature T_i ; but an attempt was made, using a gridded analyser, to look for a decrease in the normally observed ion cooling rate. A large RF component was present in the analyser signal during the heating pulse, and also during the build-up time and for some time after the end of the pulse, in spite of placing a damped crowbar circuit across the points A, B in Fig. 3. For this reason T_i measurements were taken at two times before the heating pulse and two times after it, as shown in Fig. 12. The duration of the heating pulse was chosen to be as long as possible, consistent with $n \geq n_{crit}$. A large number of shots were run with and without modulation, T_i being recorded four times in each shot. With m = 7, f = 89 kHz and b = 2.5%, no change in the cooling rate could be observed, although the ratio $\nu_{phase}/\nu_{thermal}$ was near optimum. Unfortunately, however, shot-to-shot variations caused a spread in the zero-modulation cooling rate which made this experiment marginal at best. When the frequency was increased

to 177 kHz a significant reduction of cooling rate was observed on almost every shot, although the TTMP effect here should have been smaller. Indeed the result was probably not due to TTMP at all, as was shown by going to the mode m = 1, f = 177 kHz, where similar effects were observed and TTMP would certainly have been negligible.

4. CONCLUSIONS

TTMP when applied to the PROTO-CLEO stellarator produces pump-out at a rate consistent with the theory of Stringer[6]. Electrostatic effects are also playing some part. We cannot be sure how the effect would scale to larger machines with higher plasma temperatures, although Stringer's theory predicts that the effect would be much less serious in tokamaks than in stellarators. The short energy life-time of present-day machines does imply that quite large modulations would be needed to produce an increase of ion temperature; if pump-out similar to that found in PROTO-CLEO was produced, the result would certainly be a net loss in plasma energy. Further, if the linear dependence of loss rate on modulation found in PROTO-CLEO is preserved, then the greatest heating for a given total plasma loss is obtained with short heating pulses of large amplitude, rather than the long pulses with rather small modulations which have recently been proposed for reactor heating.

There is a considerable gap in the above conclusions, namely concerning the loss rate with low mode number m, and corresponding low frequency f; it is quite possible that TTMP would be more attractive in this region. Electrostatic shielding is evidently of some importance; ideally, one would like to surround the plasma with a toroidal resistive skin, and to use single-turn coils.

5. ACKNOWLEDGEMENTS

I wish to thank D. J. Lees and the rest of the PROTO-CLEO team for help in the experiments. J. Allen was responsible for the installation of the RF supply, and R. J. Storey assisted fully with the RF design and throughout the experiments. Dr G. Cattanei (Euratom) worked on the experiment while on attachment. Finally, I thank Dr. R. J. Bickerton for useful suggestions and encouragement.

References

1. Stix, T.H., The Theory of Plasma Waves, McGraw Hill, New York (1962), p.206.
2. Canobbio, E., Nucl. Fusion 12, 561 (1972).
3. Dawson, J.M. and Uman, M.F., Nucl. Fusion, 5, 242 (1965).
4. Bolton, R.A.E., et al, Phys. Fluids, 14, 1566 (1971).
5. Lees, D.J., CLM-R 135 (1974).
6. Stringer, T.E., Symposium on Plasma Heating in Toroidal Devices, Varenna, Italy, (1974), p.178.
7. Lees, D.J., Millar, W., et al, Fifth European Conference on Controlled Fusion and Plasma Physics, 2, 135 (1972).

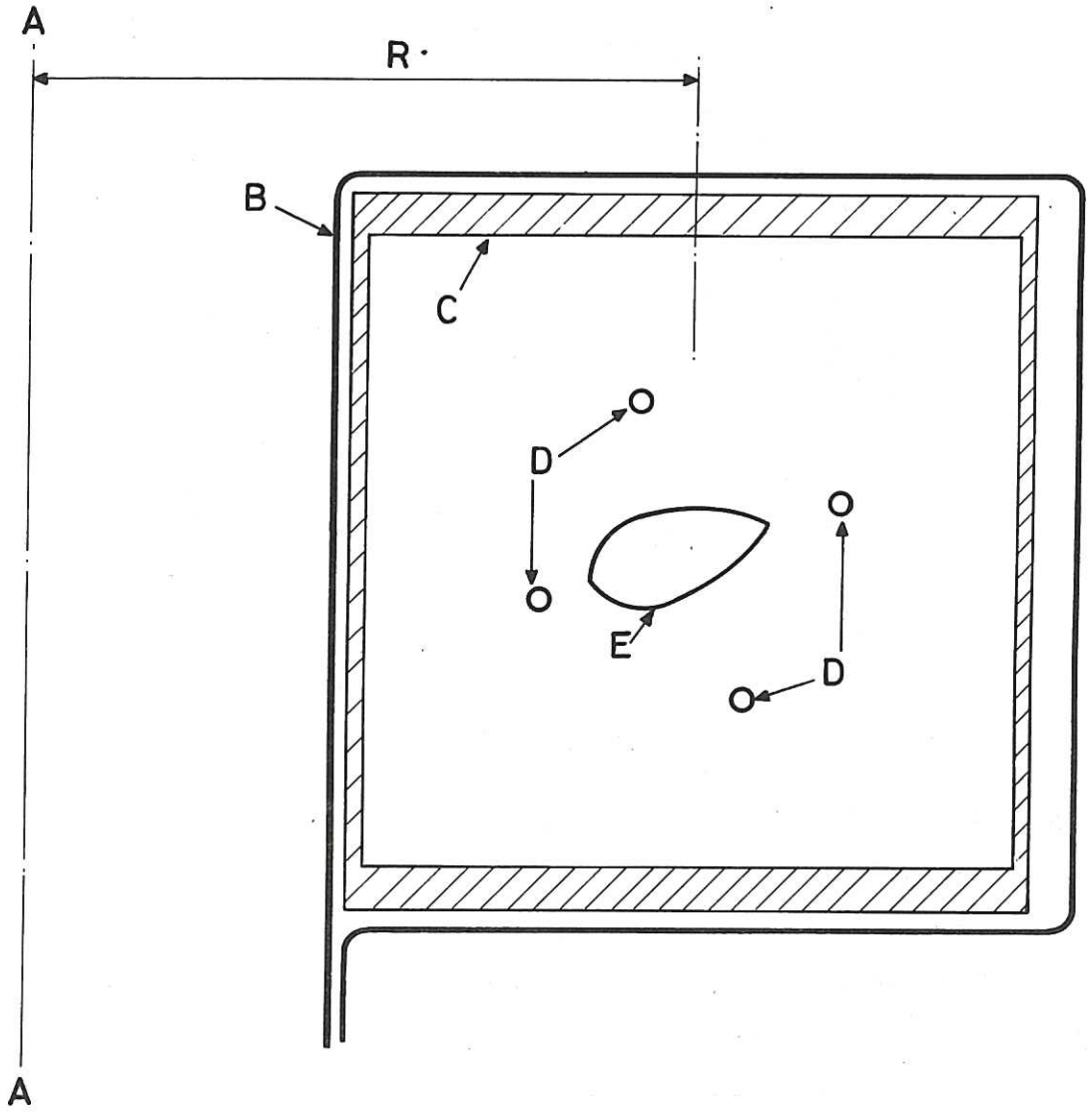

Fig.1. Section through torus of PROTO-CLEO.

A-A: major axis.

B: main field winding.

C: stainless steel vacuum tank.

D: helical winding, $\ell = 2$.

E: typical section of separatrix, $\varkappa = 0.35$ at centre.

Dimensions : R (major radius) = 400 mm.

Inside of tank: 393 mm wide by 379 mm high.

Helical conductor: 12.7 mm diameter on mean radius of 93 mm.

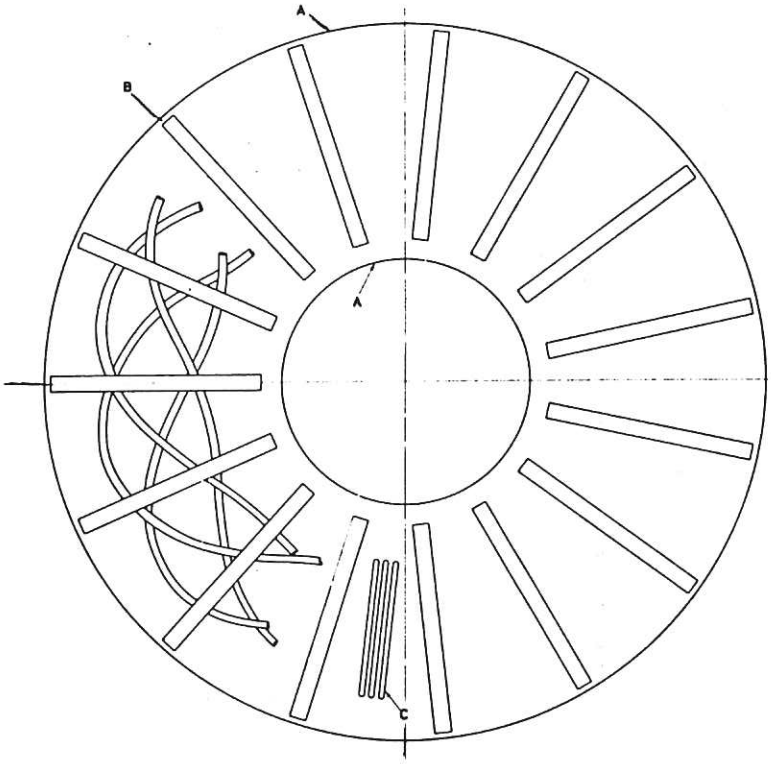

Fig. 2. Plan view of part of helical winding and supports.

A: Cylindrical walls of vacuum tank.

B: 15 equi-spaced ceramic support rings.

C: one of the 3-turn TTMP coils, separated from the helical winding by PTFE spacers.

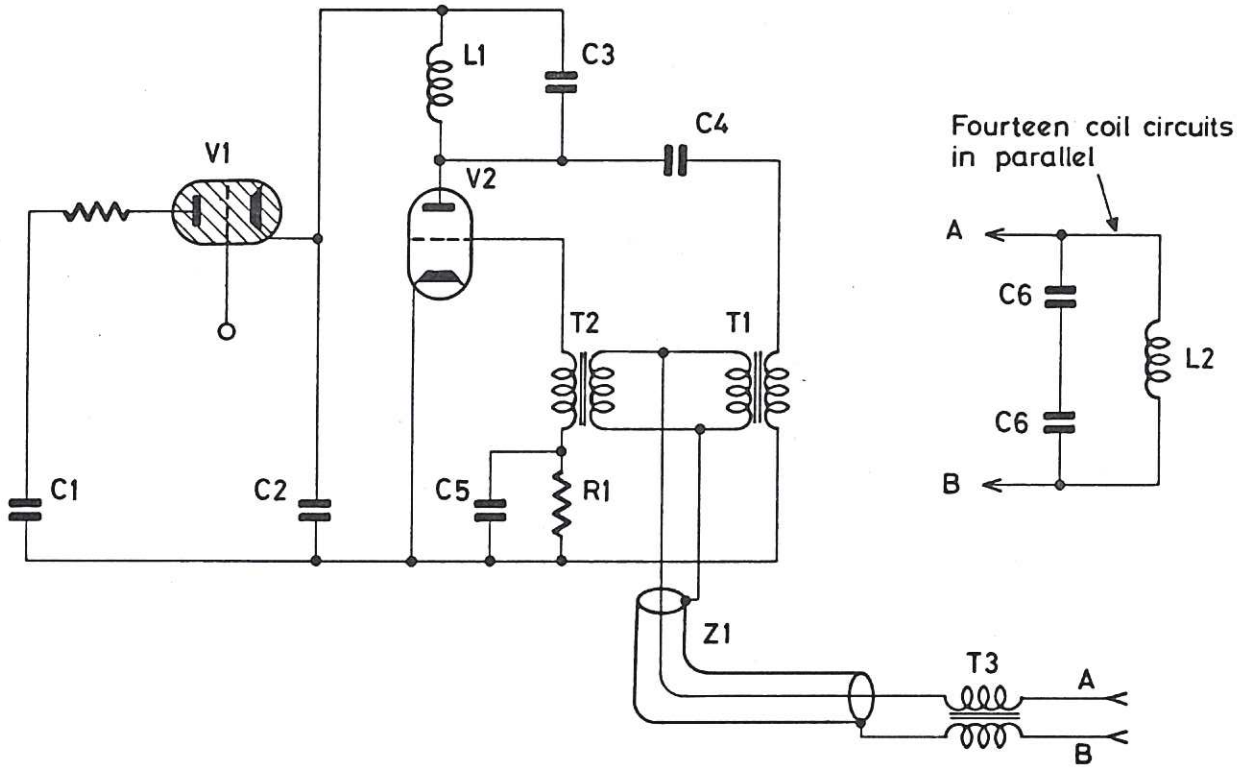

Fig. 3. Basic circuit of pulsed triode oscillator. See text for details.

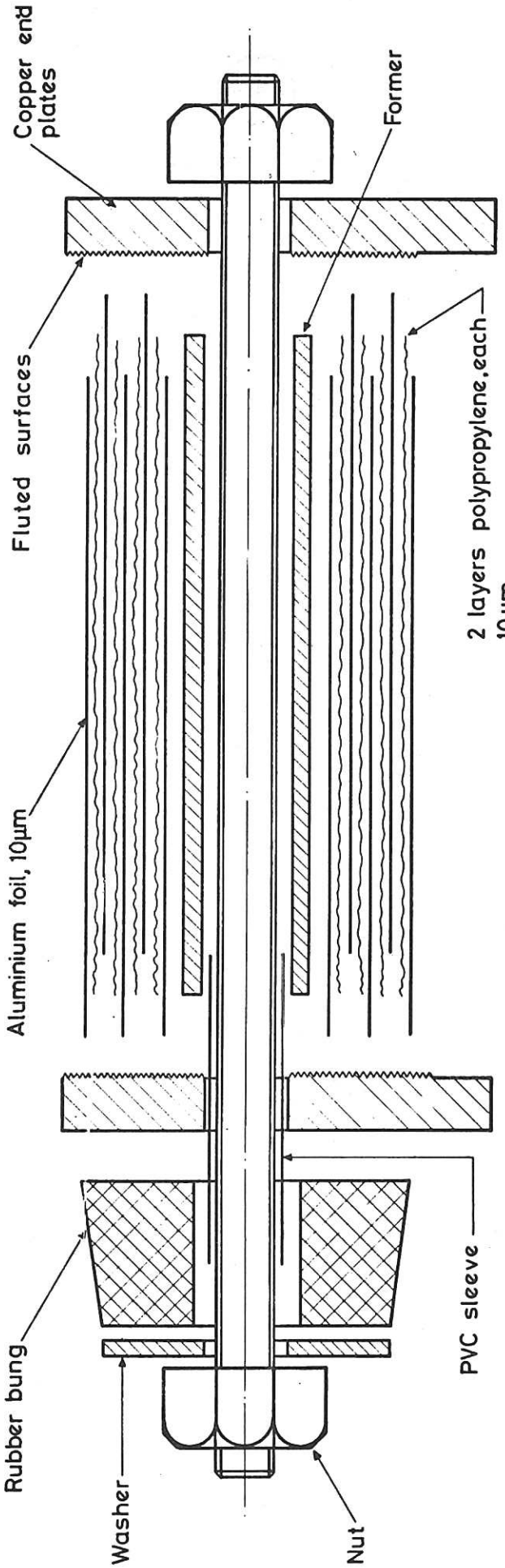

Fig. 4. Capacitor unit before tightening. The length of overlap of the two foils is 70 mm, and the diameter over the winding is 39 mm.

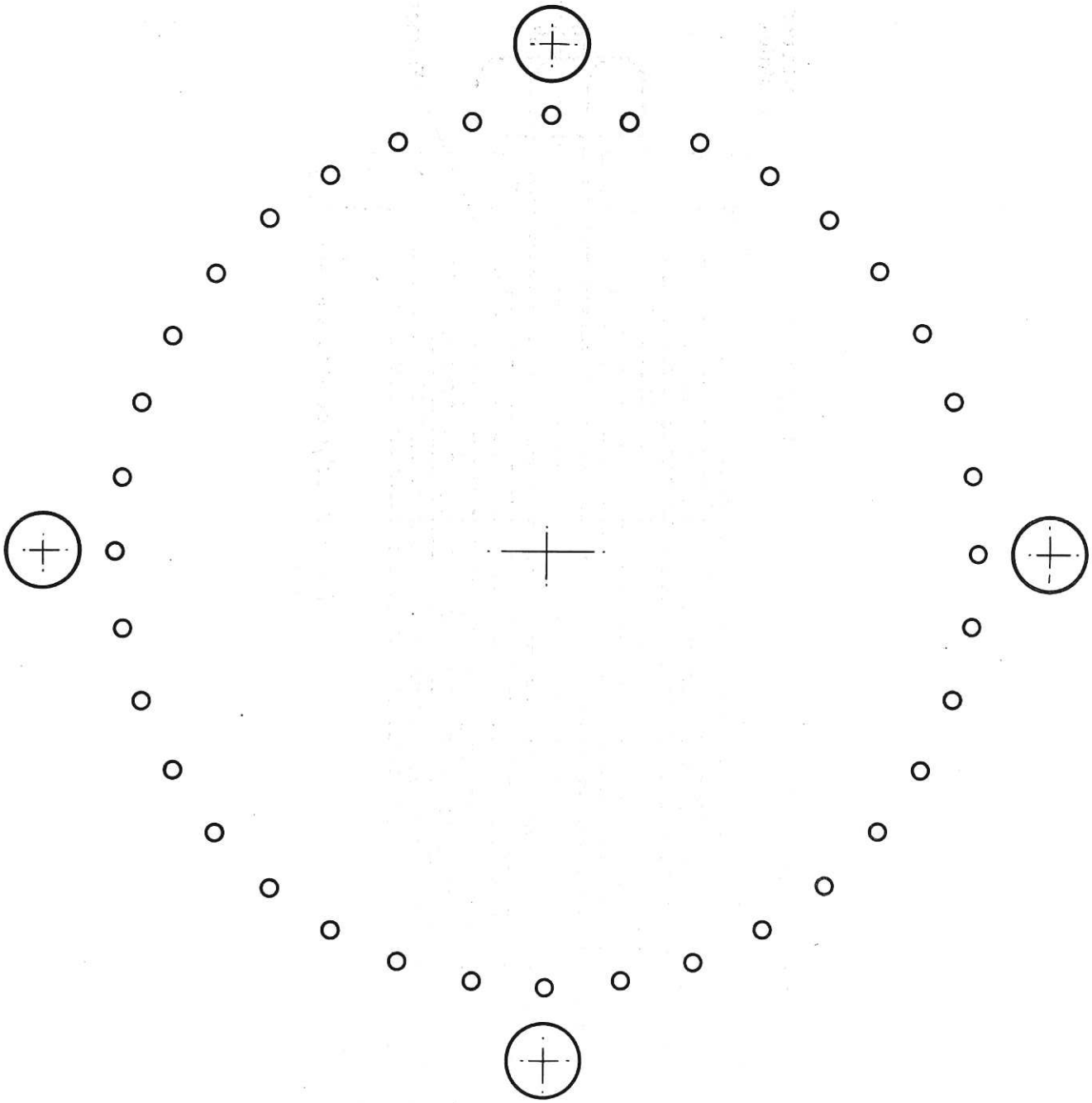

Fig. 5. A section through the $\ell = 2$ helical winding and the Faraday cage. The cage wires run parallel to the minor axis. The helical conductors have diameter 12.7 mm on a mean radius of 93 mm, and the cage wires have diameter 2.2 mm on a mean radius of 80 mm.

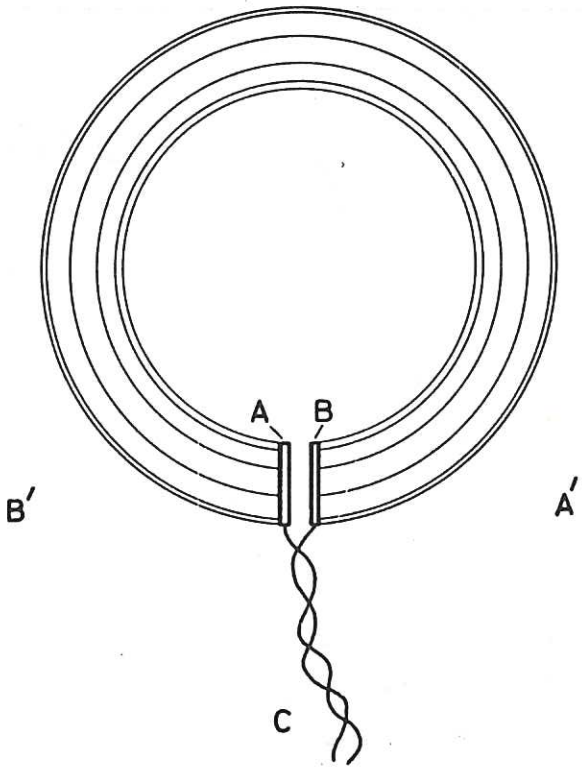

Fig. 6a. Plan view of Faraday cage. Most of the wires have been omitted for clarity. A and B are copper rings (see Fig. 6b), and C is a twisted pair of enamelled wires.

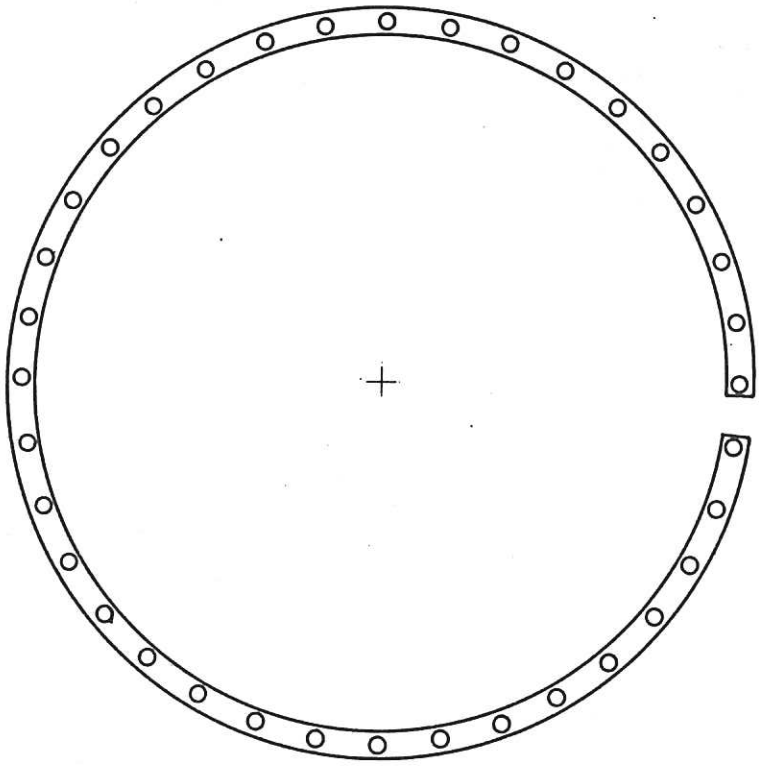

Fig. 6b. Enlarged view from A' of the copper ring A in Fig. 6a. The view of the ring B from B' is the same in reverse. The wire ends are soldered into the ring.

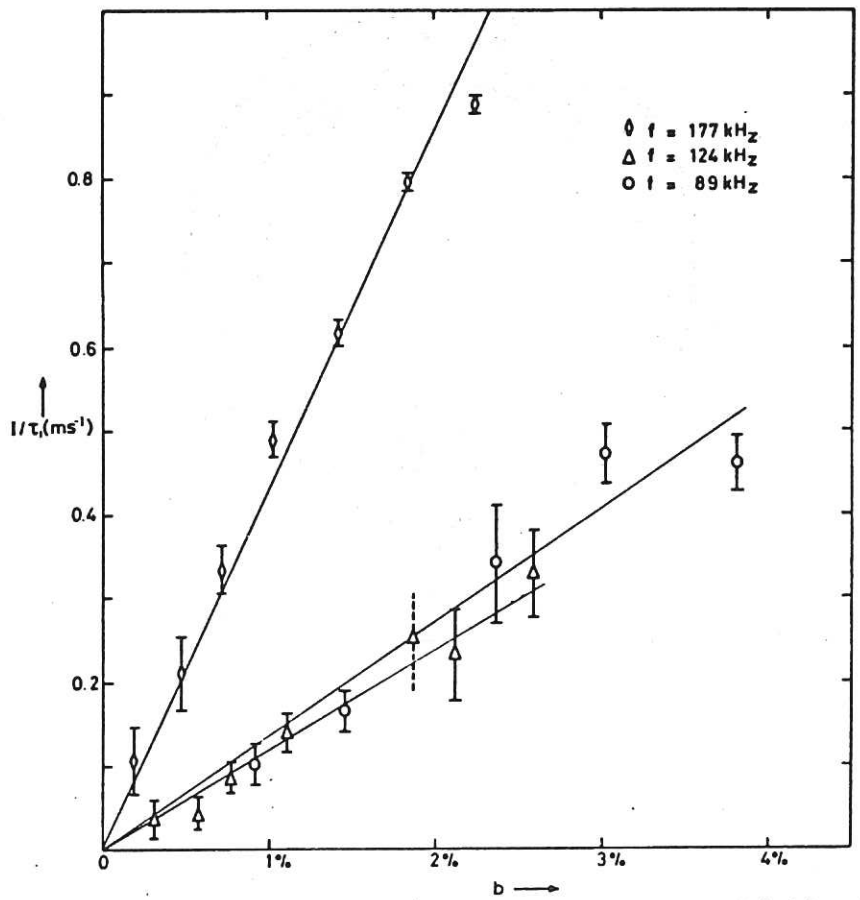

Fig. 7. Particle loss rate due to RF, $1/\tau_1$, as a function of modulation b. Taken with B_ϕ = 3 kG, m = 7, and ε = 0.35 at centre.

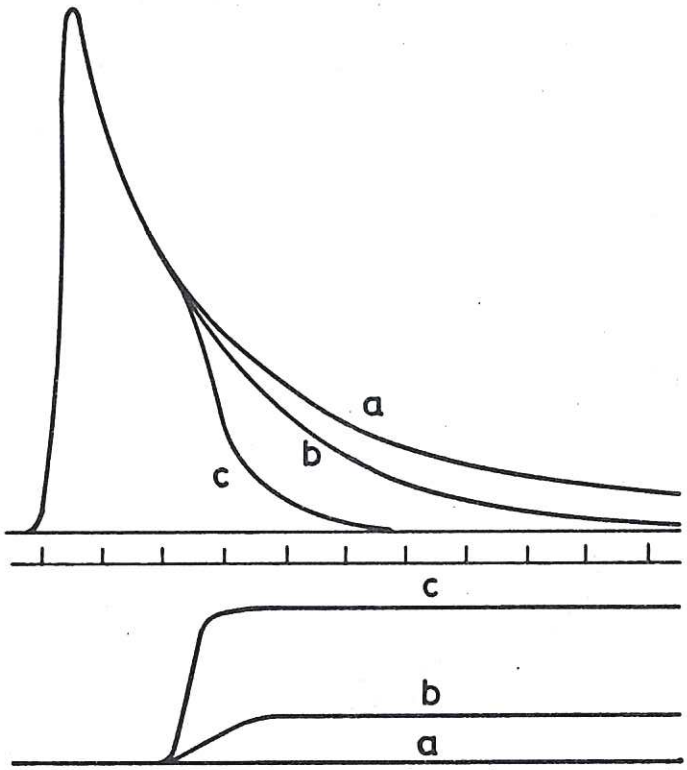

Fig. 8. General appearance of interferometer signal (upper traces). The lower traces show typical RF pulse envelopes.

(a) RF absent.

(b) Small amplitude RF.

(c) Large amplitude RF.

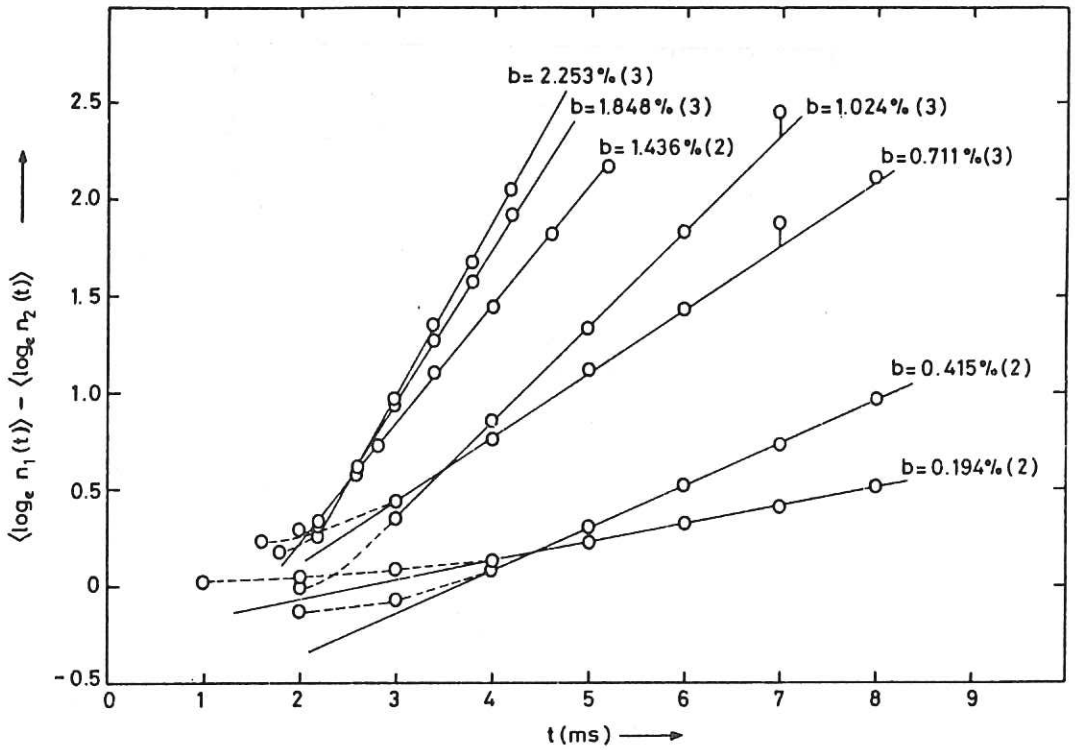

Fig. 9. Plots used in obtaining the points on the curve in Fig. 7, for f = 177 kHz. The time zero is just before plasma injection. The RF pulse is initiated just after injection; at small b values it takes longer to reach its final amplitude. The numbers in brackets denote the number of shots used in the average $\langle \log_e n_1(t) \rangle$. 8 shots were used for $\langle \log_e n_2(t) \rangle$; the spread in n_2 accounts for the fact that the plots do not diverge exactly from zero.

Similar sets of plots were used for the other two frequencies in Fig. 7.

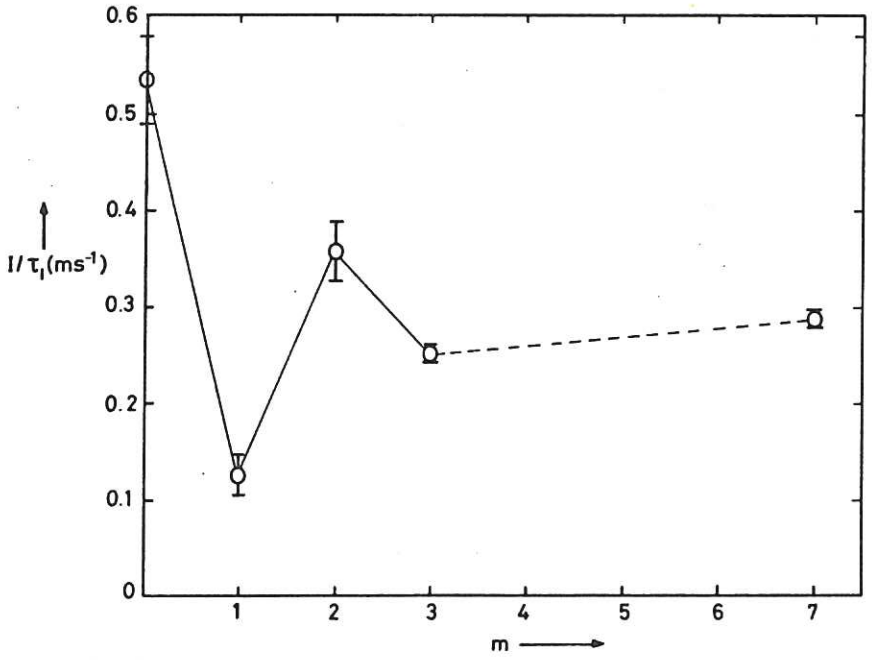

Fig. 10. Particle loss rate due to RF, $1/\tau_1$, as a function of mode number m. Taken with B_ϕ = 3 kG, $f \fallingdotseq$ 120 kHz, and x = 0.35 at centre.

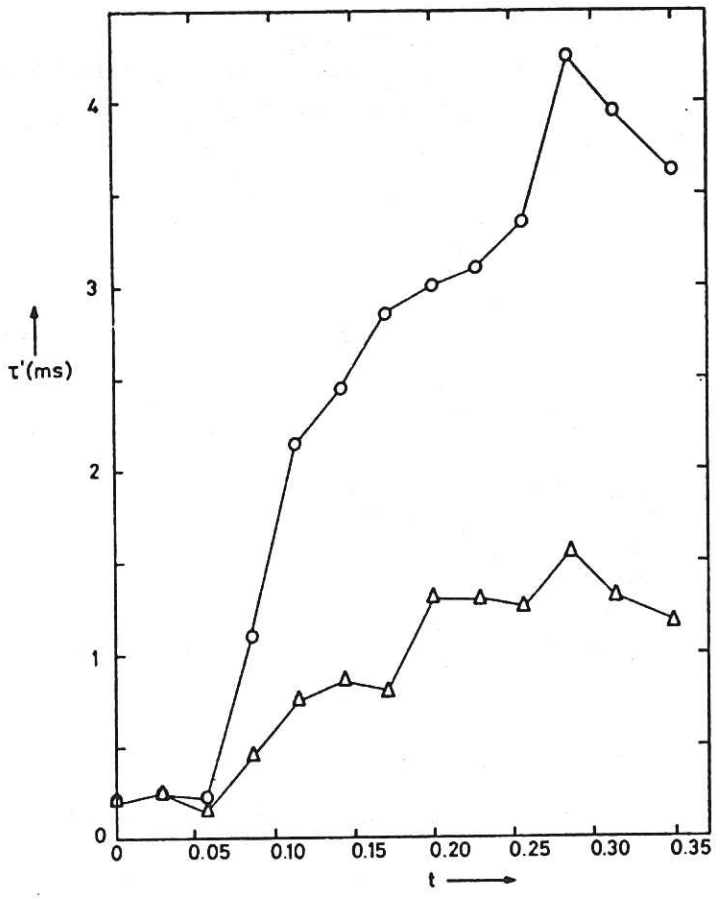

Fig. 11. Overall confinement time, τ', as a function of rotational transform, ι. Taken with B_ϕ = 3 kG, m = 7, f = 177 kHz and b = 0 (upper curve); b = 1.47 (lower curve).

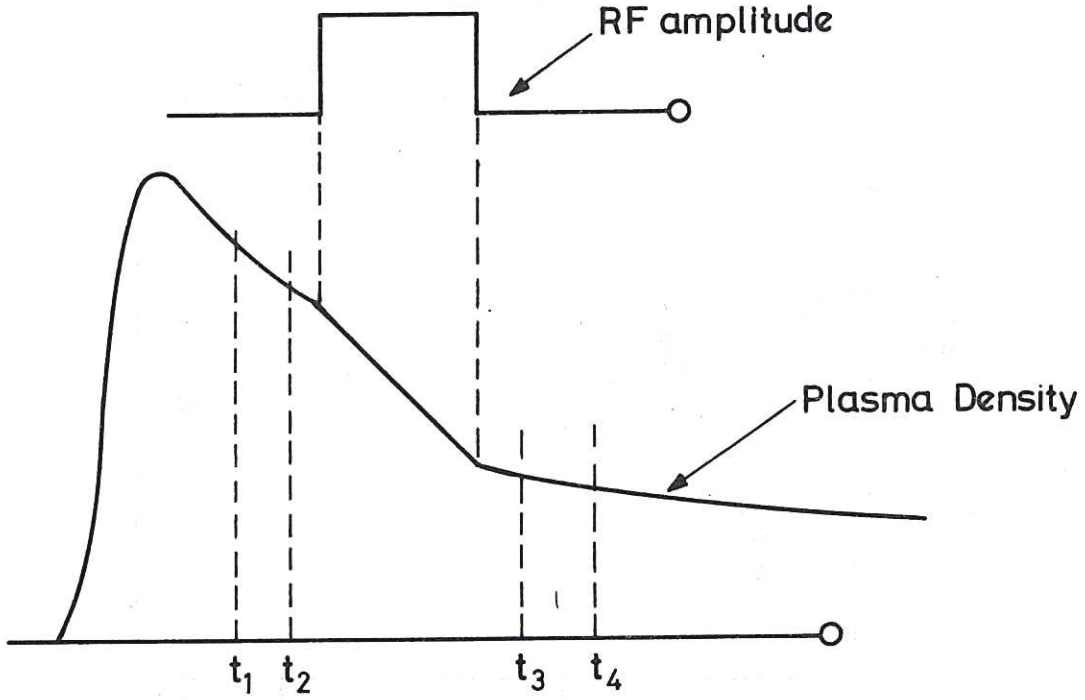

Fig. 12. Illustrating the method for ion cooling rate. T_i was measured at the four times t_1, t_2, t_3, t_4. The duration of the RF pulse was about 2 ms.

HER MAJESTY'S STATIONERY OFFICE

Government Bookshops

49 High Holborn, London WC1V 6HB
13a Castle Street, Edinburgh EH2 3AR
41 The Hayes, Cardiff CF1 1JW
Brazennose Street, Manchester M60 8AS
Wine Street, Bristol BS1 2BQ
258 Broad Street, Birmingham B1 2HE
80 Chichester Street, Belfast BT1 4JY

Government publications are also available through booksellers